A simple model for the Pauli Repulsion with possible utility in QM, MM and Chemical Education

Jordy Peeters and Kenno Vanommeslaeghe*

Department of Analytical Chemistry, Applied Chemometrics and Molecular Modelling, Vrije Universiteit Brussel

E-mail: kenno.vanommeslaeghe@vub.be

Abstract

The Pauli repulsion is the intermolecular force responsible for the volume and low compressibility of condensed-phase matter at normal conditions. A simple model for this force is presented, in which per-atom electron densities are represented as spherical charge distributions that are prevented from significantly overlapping. In the example of two noble gas atoms approaching one another beyond their van der Waals radii, the distance between the centers of the electronic charge distributions becomes larger than the distance between the nuclei, giving rise to an unfavorable electrostatic interaction. For the purpose of calculating this interaction, the model is further simplified by representing the per-atom electron density as a negative point charge, inspired by the classical Drude oscillator. The dispersion interaction is simplified to an R^{-6} term, centered on the aforementioned point charges. Despite the gross simplicity of the resulting formalism, near-quantitative agreement with high-level QM interaction energies of noble gas dimers is achieved. Accordingly, the present model is thought to have utility in force fields, in post-HF and post-DFT dispersion corrections and in chemical education.

1 Introduction

From the traditional statistical point of view, the Pauli repulsion is the only consistently repulsive force in molecular liquids. It can be said to be responsible for enforcing the van der Waals radii of the atoms, and as such, it is often cited as the force that keeps condensed-phase matter from collapsing at normal conditions. While the nature of the Pauli repulsion is well-understood at a Quantum Mechanical (QM) level, it is not straightforward to explain to an audience that lacks the requisite QM background. Perhaps more importantly, QM does not provide an analytical formula for the repulsive force as a function of the interatomic distances. In applications where such a functional form is required, approximations that are very empirical in nature are commonly employed. However, these approximations suffer from one or more of the following disadvantages: (1) computational cost (mainly in the context of condensed-phase Molecular Mechanics), (2) mediocre accuracy and (3) not being able to overcome the attractive London Dispersion at short distances in models that represent the latter force by an atom-centered R^{-6} term. Conversely, the present paper proposes a simple and elegant model for the Pauli repulsion that is straightforward to explain to a general audience and suffers from none of the aforementioned disadvantages.

To accurately classify the present model against the backdrop of the many existing models, we must start from the observations that (1) there exist two fundamentally different classes of methods to partition the electron density in a multi-atom system among its atoms and (2) any decomposition of the interatomic energy into contributions is inherently linked to a specific partitioning scheme of the electron density. Specifically, the electron density can be divided into separate atomic domains along discrete boundary planes so that the density in any region of space fully belongs to one unique atom. We will call this class of partitioning schemes the "Bader-like partitioning", after R. Bader's Atoms In Molecules theory.[1] Conversely, the electron densities belonging to the different atoms can be taken to overlap so that in a given region of space, different fractions of the density belong to different atoms. We will call this class of partitioning schemes the "Hirshfeld-like partitioning" after the seminal work of F.

Hirshfeld.[2] We now observe that for any given decomposition of the interatomic energy, the division of the total energy among different (covalent, electrostatic, dispersion, Pauli repulsion) terms is entirely reliant on the underlying scheme for partitioning the electron density. As an example, a Hirshfeld-like partitioning may give rise to an energy decomposition containing a charge penetration term,[3] while there exists no counterpart for this term in a Bader-like partitioning. Yet, both partitioning schemes can be applied to the same electron density and thus should reproduce the same interatomic forces following the Hellman-Feynman theorem. This implies that in a Bader-like partitioning, the repulsive contribution of the penetration term is incorporated into the other terms, likely including the Pauli repulsion term. Consequently, there is no uniquely correct decomposition of the interatomic energy in the same fashion as there is no uniquely correct partial charge assignment algorithm. Rather, as demonstrated at a conceptual level in the above example, two energy decomposition methods may yield different Pauli repulsion terms when viewing the same system though the framework of different density partitioning methods. While this is presumably well-known in at least part of the community, it is essential for the purpose of comparing the present work method to existing models - in particular the Pauli repulsion model of Rackers and Ponder[4] and that of Van Vleet et al.[5] Indeed, while some of the basic premises behind the two models appear somewhat similar, the work of Rackers and Ponder assumes a Hirshfeld-like partitioning and their Pauli repulsion term is used alongside a charge penetration term. Conversely, the present work consists of a simple model that is fundamentally based on a Bader-like partitioning, yielding a very different Pauli repulsion term but equally good intermolecular potentials on simple test systems. Also, while the distance-dependent Rackers and Ponder Pauli repulsion term is in line with the exchange term of a SAPT decomposition, our model is not. While this would appear worrisome at first glance, it becomes trivial in light of the dependence on the underlying partitioning scheme: SAPT treats the interatomic potential as a perturbation of a reference state that essentially consists of non-interacting spatially overlapping atoms and therefore is implicitly based on a Hirshfeld-like partitioning.

1.1 Rationale

Figure 1: A scheme in which the internuclear distance, r, and the distance between the electron clouds, r', of noble gas atoms is schematically given. In A, r' is defined as the distance between the centroids of the electron clouds. In B, r' is defined as the centroids of the outer-shell electrons.

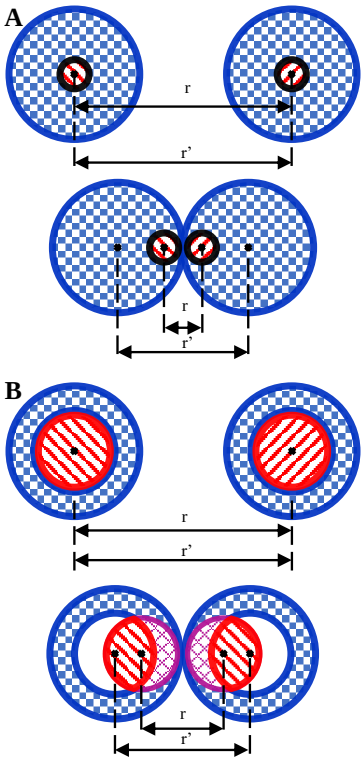

Applying a Bader-like partitioning to a simple noble gas dimer at distance $r < 2r_{vdW}$ yields per-atom electron densities that are deformed from their non-interacting shape. Most notably, the overall electron density is shifted away from the interatomic plane[4] such that a net repulsive Coulombic force is obtained, thereby satisfying the Hellman-Feynman theorem. Aiming for a thoroughly simplified model that captures this basic property, we apply a shift to the center of the spherical electron density rather than deforming it upon approach between the two atoms, as illustrated in Fig. 1A. In addition, we neglect the "tails" of the electron distribution, reducing it to a finite symmetrical sphere whose external electric field is the same as that of a point charge. This yields a model in which a noble gas dimer is reduced to a set of 4 point charges, in this respect mimicking the *classical* Drude model of polarization

as it is implemented in molecular mechanics.[6] While the Drude model features a harmonic potential to represent the attraction between a nucleus and *its own* electron density, we neglect this contribution for now; its treatment will be discussed in §1.2. Doing so reduces the interaction energy to the sum of the dispersion and Coulombic interactions:

$$E = -\frac{C_6}{r'^6} - 2\frac{C_1}{\frac{1}{2}(r+r')} + \frac{C_1}{r'} + \frac{C_1}{r} \tag{1}$$

Where r is the internuclear distance and r' is the distance between the two centers of the atomic electron densities. The C_6/r'^{-6} term represents the London dispersion interaction. Indeed, this interaction can be defined as a weakening of the electronic repulsion due to a decrease in the probability of repulsive configurations in the many-electron wave function, or expressed less formally, due to a tendency of electrons (within the total densities of the interaction partners) to "instantaneously" avoid one another. Therefore, in a model where electron densities are displaced in space, the classical r^{-6} term should trivially be centered on the electron densities rather than the nuclei, becoming an r'^{-6} term. Notably, this yields a dispersion term that is inherently immune to the common problem of divergence at short distances, because r' will not approach 0 when r does; see below. The dispersion coefficient C_6 is fitted to the potential energy surface of the interaction distance; as shown in "Results", doing so yields values that are in agreement with the literature. Finally, the three C_1 terms represent the Coulombic interactions as depicted in Fig. 1A. Naively, C_1 should simply be equal to the product of the two nuclear charges. This yielded an acceptable potential energy surface for the neon dimer, but not for larger species. Conversely, when treating C_1 as another parameter and fitting it to the potential energy surface, C_1 values were obtained that roughly approached the product of *the numbers of valence electrons* on each of the interacting atoms, suggesting that the deformation of the electron cloud is mostly limited to the valence shell!

1.2 Present model

As mentioned above and corroborated by table 4, in the context of the present formalism, the deformation of the electron clouds seems to be largely limited to the valence shell. This prompted a refinement to the naive model introduced in §1.1. The actual model that is the subject of this paper is more accurately represented by Fig. 1B, wherein r is the distance between the nuclei *along with* their immutable inner electron clouds and r' is the distance between the centers of two (isotropic) hollow shells of outer electrons. Furthermore, r' is taken to be a predetermined function of r. While this does not change the mathematical form of Eq. (1), it resolves problem of the absence of an explicit term for the attraction between a nucleus and *its own* electron density. Indeed, if the atom's "proper" electron cloud is split into a part that is always spherically symmetric around the nucleus and a second part that is a hollow sphere, its electrostatic force on the nucleus is always 0. Note that this does not imply that the mobile part of the electron cloud is allowed to move freely: instead of restraining it with an additional force, we constrain it at a position that is determined by the function r'(r), as elaborated in §1.3. This use of a constraint is conceptually analogous to the QM Pauli repulsion, which is not the result of some ghostly "QM force" acting upon the wave function, but the electrostatic consequence of the antisymmetry constraint. Interestingly, attempts to add more conventional energy terms for the interaction between a nucleus and its own electron density to Eq. (1) failed to improve the potential energy surfaces (data not shown), empirically supporting Eq. (1) as written.

1.3 The interatomic electron cloud distance

Apart from the parameters C_6 and C_1, the key undefined quantity in Eq. (1) is r'; indeed, an analytical expression of r' as a function of r is required in order to turn the above equation into a practical model. Unfortunately, deriving even an approximate analytical expression for r' from first principles is highly nontrivial. Instead, we follow the time-honored tradition of proposing a number of parametrical mathematical functions and optimizing

the newly introduced parameters to optimally reproduce high-level QM Potential Energy Surfaces. Specifically, we selected analytical functions that satisfied the following (boundary) conditions:

- At large distances, the electron cloud is centered around the nucleus, i.e. $r = r'$ Eq. (3).
- At shorter distances, around and below the sum of the van der Waals radii, r' should gradually and monotonously become larger than r.

In other words, the difference $r' - r$ should approach 0 when r approaches infinity and should monotonously increase when r becomes smaller, reaching a finite value for $r = 0$. We will henceforward define

$$f(r) := r' - r \tag{2}$$

because large parts of the mathematics that follow can be expressed somewhat more compactly and intuitively in terms of this $f(r)$. This yields:

$$\lim_{r\to\infty} r' = r \Rightarrow \lim_{r\to\infty} r' - r = \lim_{r\to\infty} f(r) = 0 \tag{3}$$

When evaluating the resulting parametrized functions, we consider an additional, somewhat less rigorous criterion for the fitness of the function. This criterion is based on the generally accepted notion that the Pauli repulsive wall becomes very steep over a very short distance range; for some intents and purposes, atoms can even be approximated as hard spheres (e.g. in the van der Waals equation of state). Accordingly, as the internuclear distance r decreases significantly below the sum of the van der Waals radii, the response of r' on the decrease in r weakens. In the present work, we will further assume that when r the approaches 0, so will $\mathrm{d}r'/\mathrm{d}r$. This is in intuitive agreement with a "hard Pauli repulsive wall" or more fundamentally with the idea that the Pauli exclusion principle enforces the antisymmetry of

the wave function as a hard constraint.

$$\left.\frac{\mathrm{d}r'}{\mathrm{d}r}\right|_{r=0} = 0 \Rightarrow \left.\frac{\mathrm{d}r'-r}{\mathrm{d}r}\right|_{r=0} = \left.\frac{\mathrm{d}f(r)}{\mathrm{d}r}\right|_{r=0} = -1 \tag{4}$$

Formulated this way, it becomes apparent that candidate functions can be constructed as

$$f(r) = a(1-\sigma(br)) \tag{5}$$

where $\sigma(x)$ is a sigmoid function in a standardised form:

$$\lim_{x\to-\infty}\sigma(x) = -1,\ \lim_{x\to+\infty}\sigma(x) = +1, \sigma(0) = 0,\ \left.\frac{\mathrm{d}\sigma(x)}{\mathrm{d}x}\right|_{x=0} = 1 \tag{6}$$

The resulting "sigmoid-based" functions automatically satisfy (3); the parameter a (or $f(0)$) can be though of as a measure for "the sum of the vdW radii of the electron clouds" and criterion (4) is satisfied when $a/b = 1$.

In the present paper, we evaluate six such "sigmoid-based" functions (7)-(12).

$$f(r) = a\left(\frac{2}{1+e^{2br}}\right) \tag{7}$$

$$f(r) = a\left(1-\frac{2}{\pi}\arctan\left(\sinh\left(\frac{\pi}{2}br\right)\right)\right) \tag{8}$$

$$f(r) = a\left(1-\frac{br}{\sqrt{1+b^2r^2}}\right) \tag{9}$$

$$f(r) = a\left(1-\frac{br}{1+|br|}\right) \tag{10}$$

$$f(r) = a\left(1-\left(\frac{\sqrt{\pi}}{2}br\right)\right) \tag{11}$$

$$f(r) = a\left(1-\frac{2}{\pi}\arctan\left(\frac{\pi}{2}br\right)\right) \tag{12}$$

In addition, polynomial functions can be made to fulfill condition (3) by introducing a cut-off distance d and eliminating the 0^{th} order term, as in (13) and (14). Note that we also

eliminated the 1st order term so that $f'(d) = 0$, ensuring a smooth transition when $f(r)$ switches to 0. This corresponds to a model where at distances $\geq d$, the electron cloud is distributed symmetrically around the nucleus and the force due to the Pauli repulsion is exactly 0. While this leaves an artificial discontinuity in the 2nd derivative, the aforementioned steepness and sudden onset of the Pauli repulsive wall suggest that it would make a very good approximation. In addition, being able to switch to a more conventional treatment beyond a given cut-off distance is highly desirable for force fields (as is the mathematical and computational convenience of a polynomial function).

$$f(r) = \begin{cases} a(r-d)^3 + b(r-d)^2 & \text{if } r \leq d \\ 0 & \text{if } r > d \end{cases} \tag{13}$$

$$f(r) = \begin{cases} a(r-d)^4 + b(r-d)^3 + c(r-d)^2 & \text{if } r \leq d \\ 0 & \text{if } r > d \end{cases} \tag{14}$$

It should be noted that, unlike the standardized sigmoid based functions (7) - (12), polynomials (13) and (14) do not automatically satisfy condition (4). Doing so requires an additional constraint, as explained in §2.2.

2 Methods

2.1 Generation of target data

Potential energy scans of the neon-neon (NeNe), argon-argon (ArAr) and argon-neon (ArNe) dimers were performed from 1.5-7.5 Å for NeNe and 2.0-7.5 Å for the other two dimers in steps of 0.1 Å using the Psi4 program.[7] To obtain a high accurate interaction energy profile, the following two point Complete Basis Set (CBS) extrapolation scheme was used (15):[8]

$$E_{total}^{\text{CBS}} = E_{total,\text{HF}}^{\text{aug-cc-pV5Z}} + E_{corl,\text{MP2}}^{\text{aug-cc-pV[Q5]Z}} + \delta_{\text{MP2}}^{\text{CCSD(T)}}|_{\text{aug-cc-pVTZ}} \quad (15)$$

Following the notation conventions from,[8] $E_{total,\text{HF}}^{\text{aug-cc-pV5Z}}$ is the Hartree-Fock energy, $E_{corl,\text{MP2}}^{\text{aug-cc-pV[Q5]Z}}$ is a correction for the CBS extrapolation and $\delta_{\text{MP2}}^{\text{CCSD(T)}}|_{\text{aug-cc-pVTZ}}$ is the correction for the level of theory. The first two terms were calculated using the Density Fitted (DF) versions of the respective algorithms but $\delta_{\text{MP2}}^{\text{CCSD(T)}}$ not (because of technical limitations). Similarly, a Counterpoise Correction was applied to the first two terms but not $\delta_{\text{MP2}}^{\text{CCSD(T)}}$, because the computational cost of doing so was not deemed worth the modest improvement in accuracy for this particular purpose. The interaction energy obtained in this fashion for internuclear distance x will henceforward be referred to as $E_{\text{QM}}(x)$

2.2 Parameter optimization

For each E_{QM} in the PES, a corresponding r'_{QM} (and hence $f_{\text{QM}}(x)$) was calculated by solving Eq. (1) for r'. For this purpose, the constant C_6 was initially fitted to the long-distance "tail" of the PES, while C_1 was taken as the product of the atomic numbers of the interacting atoms (when expressed in atomic units).

Based on (7)-(14), two sets of fitted algebraic functions were generated as candidates for $f(x)$. In the first set, the parameters (a, b and d, where applicable) were optimized to minimize $\sqrt{\langle (f(x) - f_{\text{QM}}(x))^2 \rangle}$, while the second set aimed to minimize $\sqrt{\langle w_i (E(x) - E_{\text{QM}}(x))^2 \rangle}$ using (1) for $E(x)$.

Because the range of $E(x)$ spans several orders of magnitude, it was necessary to apply weight factors: $w_i = 1$ for $E_{\text{QM}}(x) < 17$ kcal/mol and $w_i = k/E_{\text{QM}}(x)^2$ for $E_{\text{QM}}(x) > 17$ kcal/mol. For the neon dimer k was arbitrarily set to 10 and for the other dimers k was set to 1. Note that for the sake of comparison, only the points with $E_{\text{QM}}(x) < 17$ kcal/mol were used for calculating the RMS energy differences (RMSE) in Table 2 and Table 3.

In the case of the quartic function, parameter c was not optimized but instead fixed to the value given by Eq. (16) in order to satisfy the "hard Pauli repulsive wall" condition (4).

$$\left.\frac{\mathrm{d}r'}{\mathrm{d}r}\right|_{r=0} = 0 \Rightarrow c = ad^2 - \frac{3}{2}bd \tag{16}$$

The actual fitting was performed using the Differential Evolution and Particle Swarm (DEPS) algorithm as provided by the "Solver" feature in Libreoffice Calc 6.0.7. Different initial guesses were provided for each parameter optimization in order to verify that the problem was single-minimum and well-conditioned. While the process occasionally needed to be continued after reaching its time limit, robust solutions were eventually obtained in all cases.

3 Results

3.1 Fit of $r'_{\mathrm{QM}} - r$

When substituting the QM interaction energy E for a given distance r into equation (1), it can be solved for r', yielding an "ideal" r'_{QM}. The shape of the resulting graph (black curve in Fig. 2 for Ar-Ar) provided inspiration for proposing functions Eq. (7) - (14). The latter were fitted to $r'_{\mathrm{QM}} - r$ by optimizing parameters a, b and d (where applicable). C_1 and C_6 were not included in the fit but rather set to precomputed values (see "Methods") in order to minimize the risk of overfitting in this "exploratory" stage of the work.

To assess the fitness of the proposed functions, the RMSD values of $f(r)$ for NeNe, ArAr and ArNe are given in Table 1. $f(0)$ and $f'(0)$, i.e. the value of $f(r)$ and its first derivative at $r = 0$, are included in the same table for the purpose of evaluating $f(r)$'s behavior. At small distances; per Eq. 4 and the associated reasoning, $f'(0)$ should ideally be close to -1. Likewise, $f(0)$ is the minimum possible distance between the centers of the mobile parts of the electron clouds; on a conceptual level, it fulfills the role of a "sum of the van der Waals

Figure 2: Fitted function $f(r)$ targeting $r'_{\mathrm{QM}} - r$ for the argon dimer

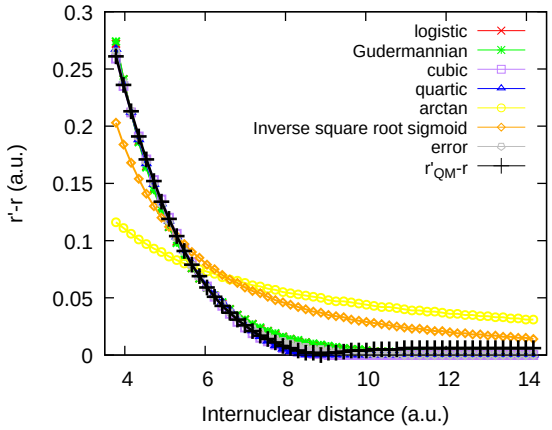

radii of the electron clouds". Based on Table 1, the inverse square root sigmoid (9), fast sigmoid (10) and arctan (12) functions perform poorly, as can readily be observed for (9) and (12) in Fig. 2. Furthermore, their RMSD values are roughly an order of magnitude higher compared to the other candidate functions. The error (11) and cubic (13) functions have low RMSD values and look acceptable in Fig. 2. However, their $f'(0)$ deviates too much from -1 in Table 1. Based on these numbers, one would expect the logistic (7), Gudermannian (8) and quartic (14) functions to be suitable. Looking at Fig. 2, (14) does especially well in the region where r'_{QM} approaches r, i.e. between 7 and 9 a.u.

Table 1: RMS deviations between the fitted function $f(r)_{\mathrm{fit}}$ and $r'_{\mathrm{QM}} - r$. Calculated $f(0)$ along with $f'(0)$, the function values and their derivatives at distance 0. All quantities are distances and are given in a.u.

Eq.	Function	neon-neon			argon-argon			argon-neon		
		RMSD	$f(0)$	$f'(0)$	RMSD	$f(0)$	$f'(0)$	RMSD	$f(0)$	$f'(0)$
7	Logistic	0.0037	1.9	-0.82	0.0060	2.0	-0.72	0.0053	1.6	-0.58
8	Gudermannian	0.0039	2.5	-1.36	0.0056	2.8	-1.21	0.0060	2.0	-0.89
9	Inv. sq. root sigm.	0.0240	2.5	-2.50	0.0268	157	-818	0.0421	11	-14.6
10	Fast sigmoid	0.0434	10	-346	0.0478	24	-1321	0.0628	44	-2901
11	Error	0.0065	1.2	-0.39	0.0040	0.50	-0.09	0.0033	1.1	-0.32
12	Arctan	0.0433	499	$-3.8 \cdot 10^5$	0.0477	263	$-1.0 \cdot 10^5$	0.0563	1003	$-1.3 \cdot 10^6$
13	Cubic	0.0047	1.1	-0.44	0.0039	1.2	-0.36	0.0037	1.1	-0.39
14	Quartic	0.0037	1.6	-1.00	0.0024	2.1	-1.00	0.0043	1.8	-1.00

Finally note that $f'(0)$ is exactly -1 for the quartic function (14) because of constraint (16). We attempted to constrain parameter b in cubic function (13) in a similar fashion, but the optimization of the remaining parameters failed to converge and yielded extremely poor

fits (data not shown). This suggests that the polynomial functions need a minimum of three parameters in order to obtain acceptable fits; this observation is discussed in more detail at the end of §3.2.

3.2 Fit of E_{QM} using precomputed C_6 and C_1

While using a "back-calculated" $r'_{\mathrm{QM}} - r$ provided a sure footing for the evaluation of the different functional forms in §3.1, it relied on precomputed values of C_6 and C_1 in addition to being mathematically somewhat cumbersome. For our final models, more flexibility was afforded by optimizing the parameters in the selected functions (7), (8) and (14) so that they optimally reproduce E_{QM} when plugged into Eq. (1). As a consistency check, this was initially performed using the same precomputed C_6 and C_1 as in §3.1. Zooming in on the the potential energy surfaces for the argon dimer in Fig. 3, the logistic (7) (red) or Gudermannian (8) (green) function led to a relatively substantial underestimation of the interaction energy, while the quartic (14) (blue) function produced a slight overestimation. The same observations hold for the neon dimer and the argon-neon complex (data not shown). Additionally, the quartic function predicts the equilibrium distance of the dimers accurately while the logistic and Gudermannian functions somewhat overestimate it. Table 2 shows that comparable $f(0)$ and $f'(0)$ values were obtained when compared to Table 1. Accordingly, the quartic function is superior based on the RMS energy differences when compared to the other two. It should be noted that the better fit of the quartic function is a natural consequence of its having three "fittable" parameters (a, b, and d, since we still use Eq. (16) for c), compared to the two (a and b) in the logistic and Gudermannian functions. Indeed, one could argue that after constraining (3) and (4), three degrees of freedom (DOF) are needed to reproduce three physical properties of $f(r)$: (I) $f(0)$, (II) the r at which $f(r)$ becomes arbitrarily small (for the polynomial functions, "arbitrarily small" can be taken as 0 and so that distance becomes d) and (III) the concavity ("sag") of $f(r)$ between $r = 0$ and $r = d$. Viewed in this framework, properties (II) and (III) are intrinsically tied together for sigmoids (7)-(12)

and only the logistic and Gudermannian functions do this in a fashion that approximates the physical $f(x)$. Conversely, the quartic function (with constraint (16)) has exactly the required freedom to fit all three properties independently.

Figure 3: Fitted potential energy functions for the argon dimer, targeting $E_{\mathrm{int,QM}}$ by optimizing only $f(r)$

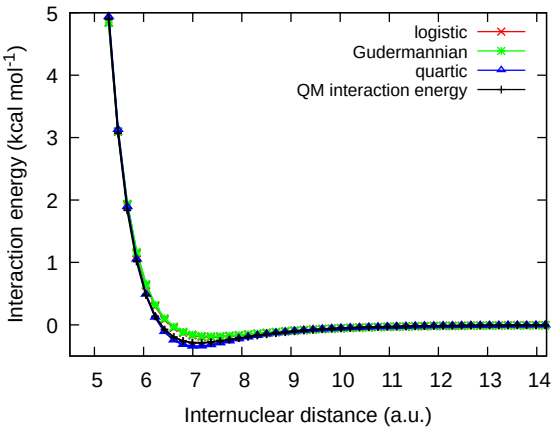

Table 2: RMS energy differences between E_{fit} with E_{QM} (in kcal/mol) computed as explained in "Methods" together with calculated values of $f(0)$ and $f'(0)$ (in a.u.), the calculated values of the functions and their derivatives at distance 0.

Eq.	Function	neon-neon			argon-argon			argon-neon		
		RMSE	$f(0)$	$f'(0)$	RMSE	$f(0)$	$f'(0)$	RMSE	$f(0)$	$f'(0)$
7	Logistic	0.0326	1.8	-0.81	0.0669	2.1	-0.77	0.0348	2.0	-0.77
8	Gudermannian	0.0441	2.5	-1.32	0.0741	2.9	-1.25	0.0562	2.5	-1.16
14	Quartic	0.0065	1.8	-1.00	0.0250	2.1	-1.00	0.0163	1.9	-1.00

3.3 Fit of $f(r)$, C_1 and C_6 to E_{QM}

Finally, the models were further relaxed by including C_1 and C_6 in the set of parameters to be fit to the QM interaction energy. As can be seen in Fig. 4 for the case of the argon dimer, this makes all three functions yield potential energy surfaces that are visually indistinguishable from the $E_{\mathrm{int,QM}}$. However, the $f(0)$ and $f'(0)$ values in Table 3 for the logistic (7) and Gudermannian (8) functions are probably overfitted with respect to the physical justification of the model, while they appear reasonable for the quartic (14) function.

Figure 4: Fitted potential energy functions for the argon dimer, targeting $E_{\mathrm{int,QM}}$ by optimizing $f(r)$, C_1 and C_6

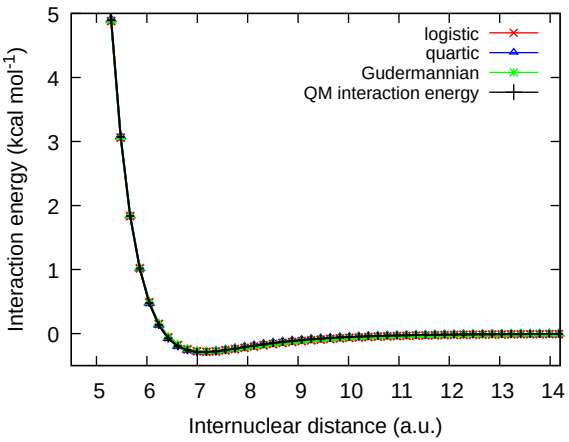

Table 3: RMS energy differences between the E_{fit} with E_{QM} in kcal/mol with C_1, C_6 and optimized $f(r)$ parameters. $f(0)$ along with $f'(0)$, the calculated derivatives at distance 0 in a.u.

Eq.	Function	neon-neon			argon-argon			argon-neon		
		RMSE	$f(0)$	$f'(0)$	RMSE	$f(0)$	$f'(0)$	RMSE	$f(0)$	$f'(0)$
7	Logistic	0.0035	4.5	-2.00	0.0101	23	-9.08	0.0057	11	-4.37
8	Gudermannian	0.0040	8.1	-4.59	0.0103	38	-19.1	0.0057	19	-9.66
14	Quartic	0.0006	1.9	-1.00	0.0027	2.7	-1.00	0.0021	2.3	-1.00

Further insights can be gained from examining the fitted C_1 and C_6 factors as given in Table 4. Using the quartic function led to an accurate reproduction of the precomputed C_6 term for all dimers, while this term is somewhat (albeit not gravely) overestimated with the logistic and Gudermannian functions. Conversely, the fitted C_1 values are far lower than the products of the nuclear charges that were used until now. It was in fact this discrepancy that led us to propose the model in Fig. 1B. In this model, C_1 (in a.u.) would be the product of the numbers of *mobile* electrons in the two interaction partners. This implies that for homodimers, the square root of C_1 should be a measure for the *effective* number of mobile electrons in the monomer.

For the models for NeNe and ArAr based on the quartic function, this yields $\sqrt{C_1}$ values of 9.0 and 10.0, respectively, which seems plausible when considering that the nonzero mobility of the inner electrons should add a modest positive correction term on top of the 8 valence shell electrons. If so, ArNe would appear to be in contradiction with our model: its C_1 is not only lower than the product of the two $\sqrt{C_1}$ values above, but also lower than that for NeNe, despite Ar being a larger and more polarizable species. When considering the logistic function, $\sqrt{C_1}$ values of 4.5 for NeNe and 2.6 for ArAr were obtained. While the product of the latter two values (12.0) is in reasonable agreement with the fitted C_1 for ArNe, the very small value for ArAr compared to the somewhat larger value for NeNe seem difficult to reconcile with physical reality. Similarly unlikely results were obtained with the Gudermannian function, in line with the earlier assessment that functions (7) and (8) are probably overfitted. On a more algebraic level, it has been pointed out at the end of §3.2 that the sigmoid functions are one DOF short of being able to perfectly fit the relevant properties of $f(r)$. In the present context, this provides the fitting algorithm with an incentive to compensate possible shortcomings in $f(r)$ with unphysical C_1 values. Conversely, the quartic function not only posesses the correct number of DOF, but its more accurate C_6 and more realistic $f(0)$ and $f'(0)$ values make it seem more likely to also yield physical C_1 values. In this light, its somewhat contradictory C_1 for ArNe may be explained by observing that Eq.

(1) is probably too simplistic for heterodimers. Indeed, in its present form, our model would likely become inaccurate if the deformabilities of the monomers differ significantly. While we see a number of ways to address this without compromising the model's conceptual simplicity, they unavoidably require a much larger training set of dimers in order for the parametrization problem to be properly determined, and therefore are beyond the scope of the present paper.

Table 4: (Pre)calculated and fitted C_1 and C_6 parameters (in a.u.) for three noble gas dimers. [a] The product of the nuclear charges was used as a calculated C_1. [b] The calculated C_6 was derived from the "tail" of the PES.

	C_1				C_6			
	calc[a]	Quartic	Logistic	Gudermannian	calc[b]	Quartic	Logistic	Gudermannian
NeNe	100	81.4	20.6	13.3	8.1	8.4	10.5	10.6
ArAr	324	99.6	7.0	6	91.4	91.1	110	111
ArNe	180	77.9	9.7	7.3	26.5	27.6	33.0	33.4

4 Discussion

4.1 Dispersion corrections for QM methods lacking correlation

The most popular post-HF and post-DFT dispersion corrections[9,10] represent the dispersion interaction as an R^{-6} energy term (occasionally augmented by higher order terms[11] and/or anisotropy[12]) that is centered on the nuclei. An important pitfall of this approach is that the magnitude of an R^{-6} function increases faster for $R \to 0$ than any other interaction in a (supra)molecular system, resulting in a collapse at short distances and artifacts at intermediate range. Accordingly, said dispersion corrections always feature a "damping function" that causes the final dispersion energy to level off at short distances. Examples of such damping functions are Becke-Johnson,[13] zero-damping/Chai-Head-Gordon[14] and Wu-Yang[15] damping function. Viewed in this context, the present work proposes way to damp post-HF and post-DFT dispersion corrections that is more "natural" in our opinion, while yielding accurate noble gas dimer interaction energies as a function of distance.

4.2 Molecular Mechanics

Over the years, many different Potential Energy Functions (PEF) for Molecular Mechanics (MM) have been proposed. However, the field of biomolecular simulations - which arguably plays a front-runner role in capturing subtle interactions using MM - until recently has been dominated by the Class I PEF, with improvements that were mainly driven by refinements of the parameter sets. Only in the 2000s, the limits of the Class I PEF started becoming tangible. Specifically, the lack of polarizability in the underlying fixed point charge model became a limiting factor for the accuracy and transferability of Class I Force Fields (FF), precipitating a sudden proliferation of polarizable biomolecular force fields.[16] The rate at which polarizable biomolecular force fields are adopted in applications studies is steady but slow due to their higher computational cost as well as the fact that they are still undergoing significant changes/improvements.[17,18] However, looking further ahead, they will eventually encounter limiting factors in their PEF too. One such factor is possibly the Pauli repulsion term. Indeed, the classical R^{-12} term of the Lennard-Jones potential leaves much to be desired.[19] Accordingly, a number of alternatives have been proposed.[5,20–23] However, none of these functional forms have found widespread popularity, owing to similar shortcomings in quality and/or computational cost. Conversely, the present model closely matches high-level QM results while being based on computationally inexpensive mathematical operations - at least in the case of functions (9), (10), (13) and (14).

4.3 Chemical education

The nature of the Pauli repulsion is often shrouded in confusion even in professional scientific discussions outside of physics and physical chemistry. Specifically, it is often pictured as a unique force with a quantum nature that has no classical equivalent. This is incorrect in the sense that the force associated with the Pauli repulsion is fundamentally electrostatic in nature, as a textbook consequence of the Hellman-Feynman theorem. Indeed, as two non-reacting molecular entities approach one another beyond the sum of their vdW radii,

the antisymmetry of the fermionic wave function requires the electron density to adapt a "less ideal" configuration that possesses a higher electrostatic energy than the sum of the non-interacting entities. It is the authors' opinion that the confusion on this matter represents a significant shortcoming in basic chemical education. We further speculate that this hiatus is caused by the fact that the established description of the Pauli repulsion as an exchange interaction is too abstract/advanced for students in a basic chemistry course, forcing educators to seek refuge in treatments that are oversimplified at best. In our opinion, the current model presents an opportunity to remedy this problem. Specifically, when discussing non-covalent interactions, it is straightforward (and important) to point out that the same Pauli exclusion principle that prevents two electrons from having the same set of quantum numbers also prevents two filled orbitals from occupying the exact same space. When two (non-reacting) atoms approach one another, this principle starts asserting itself gradually, resulting in a situation resembling the one depicted in Fig. 1. This can be expressed in words as a *fundamental limitation* of the wave function (i.e. the Pauli exclusion principle) that *requires* the electron density to deflect outward, resulting in a net repulsive electrostatic interaction.

4.4 Limitations

While the current model is appealing for its simplicity and accurate performance on noble gas homodimers, its present simplistic form is also very limited in scope. On a practical level, its most obvious shortcoming is that it is not expected to perform well when the interacting atoms are dissimilar. As discussed at the end of §3.3, extending the model to address this seems mathematically straightforward but would require a much larger training set of dimers. As the scope of the present paper is more conceptual, this will be deferred to a later publication.

On a more fundamental level, the present model remains a substantial simplification of the QM reality. First, the electron density is rather coarsely represented as a point charge

that is also the origin of a pure R^{-6} dispersion interactions. By doing this, we preclude *directly* capturing (among others) non-spherical deformations of the electron density and crowding-induced contraction of the electron clouds. Relatedly, the model in its present form would fail to account for the Pauli repulsive force that arises if an atom is approached by other atoms from several (isotropically distributed) directions at once. For the simplest case, a central noble gas atom with 2 other noble gas atoms approaching from opposite directions, one could propose to split the "classical Drude particle" on the central atoms into two (or more) such particles that avoid orbital overlap by deflecting perpendicular to the interatomic axis (similar to the two lobes of a p-orbital). This would give rise to unfavorable dipole-quadrupole interactions, tentatively restoring the validity of the model. For a larger number of surrounding atoms, this approach could be generalized to any geometrically appropriate number of Drude particles, yielding higher-order multipole moments. However, we surmise that this *modus operandi* will eventually encounter a fundamental limit. Specifically, under uniform compression, the volumetric confinement of the wave function (and the accompanying rise in zero-point energy) will start contributing significantly to the observed repulsion. This effect is completely absent from the current model, underlining its approximate nature.

Viewed in this light, the model probably performs as well as it does by implicitly recovering some physical phenomena through the parametrization of the function $f(r)$. It is our opinion that this is not a fundamental problem for the applications listed above. Indeed, cancellation of error through parametrization is the "default *modus operandi*" in the Force Field world and can reasonably be assumed to play a significant role in the success of post-HF and post-DFT dispersion corrections. As for the context of chemical education, the utility of the present model is essentially limited to the fundamental notion of electron clouds being *constrained* to avoid one another, giving rise to an unfavorable electrostatic interaction, regardless of the specific choices of representing the electron clouds as point charges and describing their mutual avoidance mathematically with a function $f(r)$. Nevertheless, we anticipate that these very crude and simplistic choices cannot entirely be upheld when applied to molecules

and supramolecular assemblies in the condensed phase.

5 Conclusions

We have presented a novel model for the Pauli repulsion that is intuitively accessible to audiences with little QM background, possibly encouraging a more accurate general understanding of the physical basis of this important phenomenon in these audiences. Combined with additional simplifications, it yields a simple and computationally inexpensive formalism for the empirical treatment of the van der Waals interactions in computational chemistry. While this formalism is able to closely reproduce high-level QM interaction energies of noble gas dimers, we anticipate that some of the aforementioned simplifications - most notably the use of a single point charge per atom - will need to be abandoned to be generally applicable to condensed phase molecular systems, in agreement with existing models.[4,24] Additionally, it should be emphasized that the present model is not meant to comprehensively capture the quantum mechanical reality behind the Pauli repulsion. Rather, we present it as an alternative to existing approximate models. In this capacity, it can potentially be employed in future force fields as well as post-HF and post-DFT dispersion corrections. Doing so will require building and validating an extended version of the present model with support for dissimilar atoms. This will be the subject of future work.

Acknowledgement

This work is supported by the VUB through research council (OZR) starting funds (OZR2893, to Kenno Vanommeslaeghe). The supercomputing resources and services used in this work were provided by the VUB and the VSC (Flemish Supercomputer Center), the latter being funded by the FWO (Research Foundation - Flanders) and the Flemish Government.

Data Availability Statement

The data that support the findings of this study are available from the corresponding author upon reasonable request.

References

(1) Bader, R. F. W. Atoms in molecules. *Accounts of Chemical Research* **1985**, *18*, 9–15.

(2) Hirshfeld, F. L. Bonded-atom fragments for describing molecular charge densities. *Theoretica Chimica Acta* **1977**, *44*, 129–138.

(3) Rackers, J. A.; Wang, Q.; Liu, C.; Piquemal, J.-P.; Ren, P.; Ponder, J. W. An optimized charge penetration model for use with the AMOEBA force field. *Phys. Chem. Chem. Phys.* **2017**, *19*, 276–291.

(4) Rackers, J. A.; Ponder, J. W. Classical Pauli repulsion: An anisotropic, atomic multipole model. *The Journal of Chemical Physics* **2019**, *150*, 084104.

(5) Van Vleet, M. J.; Misquitta, A. J.; Stone, A. J.; Schmidt, J. R. Beyond Born–Mayer: Improved Models for Short-Range Repulsion in ab Initio Force Fields. *Journal of Chemical Theory and Computation* **2016**, *12*, 3851–3870, PMID: 27337546.

(6) Anisimov, V. M.; Lamoureux, G.; Vorobyov, I. V.; Huang, N.; Roux, B.; MacKerell, A. D. Determination of Electrostatic Parameters for a Polarizable Force Field Based on the Classical Drude Oscillator. *Journal of Chemical Theory and Computation* **2005**, *1*, 153–168.

(7) Smith, D. G. A. et al. PSI4 1.4: Open-source software for high-throughput quantum chemistry. *The Journal of Chemical Physics* **2020**, *152*, 184108.

(8) Halkier, A.; Helgaker, T.; Jørgensen, P.; Klopper, W.; Olsen, J. Basis-set convergence of the energy in molecular Hartree–Fock calculations. *Chemical Physics Letters* **1999**, *302*, 437–446.

(9) Grimme, S. Semiempirical GGA-type density functional constructed with a long-range dispersion correction. *Journal of Computational Chemistry* **2006**, *27*, 1787–1799.

(10) Tkatchenko, A.; Scheffler, M. Accurate Molecular Van Der Waals Interactions from Ground-State Electron Density and Free-Atom Reference Data. *Phys. Rev. Lett.* **2009**, *102*, 073005.

(11) Grimme, S.; Antony, J.; Ehrlich, S.; Krieg, H. A consistent and accurate ab initio parametrization of density functional dispersion correction (DFT-D) for the 94 elements H-Pu. *The Journal of Chemical Physics* **2010**, *132*, 154104.

(12) Grimme, S.; Hansen, A.; Brandenburg, J. G.; Bannwarth, C. Dispersion-Corrected Mean-Field Electronic Structure Methods. *Chemical Reviews* **2016**, *116*, 5105–5154.

(13) Johnson, E. R.; Becke, A. D. A post-Hartree-Fock model of intermolecular interactions: Inclusion of higher-order corrections. *The Journal of Chemical Physics* **2006**, *124*, 174104.

(14) Chai, J.-D.; Head-Gordon, M. Long-range corrected hybrid density functionals with damped atom–atom dispersion corrections. *Phys. Chem. Chem. Phys.* **2008**, *10*, 6615–6620.

(15) Wu, Q.; Yang, W. Empirical correction to density functional theory for van der Waals interactions. *The Journal of Chemical Physics* **2002**, *116*, 515–524.

(16) Vanommeslaeghe, K.; Guvench, O.; MacKerell, A. D. J. Molecular Mechanics. *Curr Pharm Des* **2014**, *20*, 3281–92.

(17) Zhang, C.; Lu, C.; Jing, Z.; Wu, C.; Piquemal, J.-P.; Ponder, J. W.; Ren, P. AMOEBA Polarizable Atomic Multipole Force Field for Nucleic Acids. *Journal of Chemical Theory and Computation* **2018**, *14*, 2084–2108, doi: 10.1021/acs.jctc.7b01169.

(18) Lin, F.-Y.; Huang, J.; Pandey, P.; Rupakheti, C.; Li, J.; Roux, B.; MacKerell, A. D. J. Further Optimization and Validation of the Classical Drude Polarizable Protein Force Field. *Journal of Chemical Theory and Computation* **2020**, *16*, 3221–3239, doi: 10.1021/acs.jctc.0c00057.

(19) Lennard-Jones, J. E. Cohesion. *Proceedings of the Physical Society* **1931**, *43*, 461.

(20) Mie, G. Zur kinetischen Theorie der einatomigen Körper. *Annalen der Physik* **1903**, *316*, 657–697.

(21) Born, M.; Mayer, J. E. Zur Gittertheorie der Ionenkristalle. *Zeitschrift für Physik* **1932**, *75*, 1–18.

(22) Buckingham, R. A.; Lennard-Jones, J. E. The classical equation of state of gaseous helium, neon and argon. *Proceedings of the Royal Society of London. Series A. Mathematical and Physical Sciences* **1938**, *168*, 264–283.

(23) Kihara, T. Virial Coefficients and Models of Molecules in Gases. *Rev. Mod. Phys.* **1953**, *25*, 831–843.

(24) Harder, E.; Anisimov, V. M.; Vorobyov, I. V.; Lopes, P. E. M.; Noskov, S. Y.; MacKerell, A. D.; Roux, B. Atomic Level Anisotropy in the Electrostatic Modeling of Lone Pairs for a Polarizable Force Field Based on the Classical Drude Oscillator. *Journal of Chemical Theory and Computation* **2006**, *2*, 1587–1597.

TOC Graphic